# Two Modes of Binding of *N*-Hydroxyguanidines to NO Synthases: First Evidence for the Formation of Iron−*N*-Hydroxyguanidine Complexes and Key Role of Tetrahydrobiopterin in Determining the Binding Mode†

David Lefèvre-Groboillot,‡ Yves Frapart,‡ Alain Desbois,§ Jean-Luc Zimmermann,|| Jean-Luc Boucher,‡ Antonius C. F. Gorren,⊥ Bernd Mayer,⊥ Dennis J. Stuehr,@ and Daniel Mansuy*,‡

*Laboratoire de Chimie et Biochimie Pharmacologiques et Toxicologiques, UMR 8601 CNRS, Université Paris 5, 45 rue des Saints-Pères, 75270 Paris Cedex 06, France, Section de Biophysique des Protéines et des Membranes, Département de Biologie Cellulaire et Moléculaire, CEA et URA 2096 CNRS, CEA Saclay, 91191 Gif-sur-Yvette Cedex, France, Section de Bioénergétique, Département de Biologie Cellulaire et Moléculaire, CEA Saclay, 91191 Gif-sur-Yvette Cedex, France, Department of Immunology, Lerner Research Institute, Cleveland Clinic Foundation, Cleveland, Ohio 44195, and Institut für Pharmakologie und Toxikologie, Karl-Franzens-Universität Graz, Universitätsplatz 2, 8010 Graz, Austria*

*Received November 25, 2002; Revised Manuscript Received February 6, 2003*

ABSTRACT: The interaction of various *N*-alkyl- and *N*-aryl-*N*′-hydroxyguanidines with recombinant NOS containing or not containing tetrahydrobiopterin ($BH_4$) was studied by visible, electronic paramagnetic resonance (EPR), and resonance Raman (RR) spectroscopy. *N*-Hydroxyguanidines interact with the oxygenase domain of $BH_4$-free inducible NOS ($BH_4$-free $iNOS_{oxy}$), depending on the nature of their substituent, with formation of two types of complexes that are characterized by peaks around 395 (type I) and 438 nm (type II′) during difference visible spectroscopy. The complex formed between $BH_4$-free $iNOS_{oxy}$ and *N*-benzyl-*N*′-hydroxyguanidine **1** (type II′) exhibited a Soret peak at 430 nm, EPR signals at $g = 1.93$, 2.24, and 2.38, and RR bands at 1374 and 1502 $cm^{-1}$ that are characteristic of a low-spin hexacoordinated Fe(III) complex. Analysis of its EPR spectrum according to Taylor's equations indicates that the cysteinate ligand of native $BH_4$-free $iNOS_{oxy}$ is retained in that complex. Similar iron(III)−ligand complexes were formed upon reaction of **1** and several other *N*-hydroxyguanidines with $BH_4$-free full-length iNOS and $BH_4$-free $nNOS_{oxy}$. However, none of the tested *N*-hydroxyguanidines were able to form such iron(III)−ligand complexes with $BH_4$-containing $iNOS_{oxy}$, indicating that a major factor involved in the mode of binding of *N*-hydroxyguanidines to NOS is the presence (or absence) of $BH_4$ in their active site. Another factor that plays a key role in the mode of binding of *N*-hydroxyguanidines to NOS is the nature of their substituent. The *N*-hydroxyguanidines bearing an *N*-alkyl substituent exclusively or mainly led to type II′ iron−ligand complexes. Those bearing an *N*-aryl substituent mainly led to type II′ complexes, even though some of them exclusively led to type I complexes. Interestingly, the $K_s$ values calculated for $BH_4$-free $iNOS_{oxy}$−*N*-hydroxyguanidine complexes were always lower when their substituents bore an aryl group (140−420 $\mu$M instead of 1000−3900 $\mu$M), suggesting the existence of $\pi-\pi$ interactions between this group and an aromatic residue of the protein. Comparison of the spectral and physicochemical properties of the *N*-hydroxyguanidine complexes of $BH_4$-free $iNOS_{oxy}$ (type II′) with those of the previously described corresponding complexes of microperoxidase (MP-8) suggests that, in both cases, *N*-hydroxyguanidines bind to iron(III) via their oxygen atom after deprotonation or weakening of the O−H bond. The aforementioned results are discussed in relation with recent data about the transient formation of iron−product intermediates during the catalytic cycle of L-arginine oxidation by eNOS. They suggest that *N*-hydroxyguanidines could constitute a new class of good ligands of heme proteins.

Nitric oxide (NO) is involved in many physiological functions, including immune response, neurotransmission, and vascular tone regulation (*1*). Its biosynthesis involves homodimeric monooxygenases called NO synthases (NOSs)[1] (*2*, *3*). Three NOS isoforms have been characterized in mammals: nNOS, which was first isolated from neurons, iNOS, an inducible NOS first found in macrophages, and eNOS, which was initially detected in endothelial cells. They all catalyze the two-step oxidation of L-arginine to L-citrulline and NO, with consumption of 1.5 mol of NADPH and 2

† This work was supported by the French Ministry of Research (fellowship grant to D.L.-G.), by National Institutes of Health Grant CA 53914 to D.J.S., and by Austrian Science Foundation (P13586-MED) and HFSP (RGP0026/2001-M) grants to A.C.F.G.

* To whom correspondence should be addressed. Telephone: 33 (0)1 42 86 21 87. Fax: 33 (0)1 42 86 83 87. E-mail: Daniel.Mansuy@biomedicale.univ-paris5.fr.

‡ Université Paris 5.

§ Département de Biologie Cellulaire et Moléculaire, CEA et URA 2096 CNRS, CEA Saclay.

|| Département de Biologie Cellulaire et Moléculaire, CEA Saclay.

⊥ Karl-Franzens-Universität Graz.

@ Cleveland Clinic Foundation.

[1] Abbreviations: $BH_4$, (6*R*)-5,6,7,8-tetrahydro-L-biopterin; DTT, dithiothreitol; EPR, electron paramagnetic resonance; Hepes, *N*-(2-hydroxyethyl)piperazine-*N*′-2-ethanesulfonic acid; ImH, imidazole; MP-8, microperoxidase-8; NOHA, $N^{\omega}$-hydroxy-L-arginine; NOS, nitric oxide synthase; $nNOS_{oxy}$, $iNOS_{oxy}$, and $eNOS_{oxy}$, oxygenase domains of neuronal, inducible, and endothelial NOS, respectively; RR, resonance Raman.

10.1021/bi0272407 CCC: $25.00 
Published on Web 03/13/2003

Table 1: Characteristics of the Visible Spectra Obtained upon Interaction of $BH_4$-Free $iNOS_{oxy}$ with N-Substituted *N*′-Hydroxyguanidines, R−NH−C(═NOH)−$NH_2$, at pH 7.4

| | | difference spectra | | | absolute spectra |
|---|---|---|---|---|---|
| | R | spectrum type,[a] $\lambda_{max}/\lambda_{min}$ (nm) | $K_s$[b] ($\mu$M) | $\Delta A_{max}$[c] ($mM^{-1}$ $cm^{-1}$) | $\lambda_{sat}$[d] (nm) |
| **1** | $C_6H_5-CH_2$ | II′, 437/400 | 140 ± 30 | 38 ± 3 | 430 |
| **2** | 4-HO−$C_6H_4$ | II′, 438/413 | 390 ± 50 | 19 ± 3 | 424 |
| **3** | 4-$CH_3O$−$C_6H_4$ | II′, 438/413 | 290 ± 40 | 18 ± 2 | 424 |
| **4** | *n*-$C_5H_{11}$ | II′, 437/414 | 1000 ± 210 | 23 ± 4 | 427 |
| **5** | H | II′, 437/408 | 3900 ± 600 | 29 ± 5 | 424 |
| **6** | 4-tBu−$C_6H_4$ | I, 389/423 | 200 ± 50 | 33 ± 5 | 397 |
| **7** | 4-$CF_3$−$C_6H_4$ | I, 393/425 | 420 ± 160 | 35 ± 6 | 398 |
| **8** | 4-Cl−$C_6H_4$ | I and II′, 392 (M) and 440 (m)/424 | ≈200 | type I, 26 ± 3<br>type II′, 3 ± 2 | 400 |
| **9** | 4-$CH_3$−$C_6H_4$ | II′ and I, 442 (M) and 392 (m)/419 | ≈300 | type II′, 19 ± 10<br>type I, 5 ± 4 | 422 |
| **10** | *n*-$C_4H_9$ | II′ and I, 436 (M) and 392 (m)/417 | ≈1100 | type II′, 18 ± 4<br>type I, 5 ± 2 | 425 |
| **11** | *n*-$C_6H_{13}$ | II′ and I, 437 (M) and 390 (m)/418 | ≈1100 | type II′, 14 ± 3<br>type I, 8 ± 2 | 424 |

[a] Type I difference spectra are characterized by a peak ($\lambda_{max}$) around 390 nm and a trough ($\lambda_{min}$) around 425 nm (*22*). Type II′ difference spectra are characterized by a peak around 439 nm and a trough around 410 nm. M denotes the main peak and m the minor peak. [b] $K_s$ values were calculated from the difference spectra obtained after the addition of increasing amounts of compounds **1**−**11** to 0.7 $\mu$M $iNOS_{oxy}$ in Hepes buffer (pH 7.4) under the conditions described in Materials and Methods. When the observed spectrum displayed several maxima, the indicated $K_s$ value is only the concentration producing half of the maximum amplitude of the difference spectrum. [c] $\Delta A_{max}$ is the maximum absorbance observed between $\lambda_{max}$ and $\lambda_{min}$ at saturating ligand concentrations. When the observed spectrum displayed several maxima, the indicated $\Delta A_{max}$ value is underestimated because of the peak and valley overlap. [d] $\lambda_{sat}$ is the position of the Soret peak observed for the absolute spectrum of the enzyme sample after addition of excess ligand (10 times the calculated $K_s$). Means ± the standard deviation from at least three experiments.

mol of $O_2$. The first step is a classical monooxygenation of L-arginine leading to $N^{\omega}$-hydroxy-L-arginine (NOHA), whereas the second step involves an oxidative cleavage of the C═NOH bond of NOHA with formation of L-citrulline and NO (*4*, *5*). These reactions occur in the homodimeric N-terminal NOS domain called the NOS oxygenase domain ($NOS_{oxy}$) which contains two cofactors per monomer, the heme (iron−protoporphyrin IX) and (6*R*)-5,6,7,8-tetrahydro-L-biopterin ($BH_4$) (*6*, *7*). Electrons from NADPH are provided by a flanking C-terminal reductase domain.

We have recently shown that NOSs were also able to catalyze the oxidation of several *N*-aryl- and *N*-alkyl-*N*′-hydroxyguanidines with formation of the corresponding ureas and NO (*8*−*10*). Since selective NO formation from the oxidation of *N*-hydroxyguanidines is a unique property of NOS, it was important to determine the mode of interaction of the *N*-hydroxyguanidines in the NOS active site. From the X-ray structures recently published for the complexes of NOHA with the oxygenase domain of iNOS and eNOS, it appears that the *N*-hydroxyguanidine moiety of NOHA is roughly parallel to the heme plane and held ∼4 Å above this plane via a strong interaction with a highly conserved glutamate residue of the protein (*11*). This positioning of the *N*-hydroxyguanidine moiety of NOHA relative to the heme is very similar to that of the guanidine moiety of L-arginine itself in the NOS−L-arginine complexes (*6*, *7*). Interestingly, the X-ray structure of $eNOS_{oxy}$ with *N*-(4-chlorophenyl)-*N*′-hydroxyguanidine showed a similar positioning of the *N*-hydroxyguanidine moiety of this compound in the $eNOS_{oxy}$ active site (*12*). On the basis of the available data for complexes of NOS with *N*-hydroxyguanidines, it thus appears that only one binding mode with an almost parallel orientation of the heme and the *N*-hydroxyguanidine moiety which is bound to protein residues was observed so far.

However, we have recently shown that *N*-alkyl- and *N*-aryl-*N*′-hydroxyguanidines act as iron ligands of microperoxidase (MP-8) (*13*). They strongly bind to the MP-8−Fe(III) complex via the oxygen atom of their C═NOH moiety in the *trans* position to the histidine axial ligand of MP-8. These data suggested that *N*-hydroxyguanidines could act as axial ligands of iron in heme proteins.

We therefore undertook a detailed study of the interactions of several *N*-aryl- and *N*-alkyl-*N*′-hydroxyguanidines with NOSs containing or not containing $BH_4$, by UV−visible, EPR, and RR spectroscopy. Our results show that *N*-hydroxyguanidines bind to $BH_4$-free NOS in two different manners. The first binding mode is the one found in the NOS−NOHA complex, the roughly parallel orientation of the heme and of their *N*-hydroxyguanidine moiety allowing dioxygen binding to the iron and oxidation of this moiety. They may also bind as axial ligands of the NOS iron in a manner similar to that previoulsy found for MP-8. The structure of their aryl (or alkyl) substituent and the presence of $BH_4$ play critical roles in the choice between these two binding modes.

## MATERIALS AND METHODS

*Chemicals and Reagents.* DTT, Hepes, and ImH came from Sigma Biochemicals. $BH_4$ was purchased from Alexis Biochemicals (Coger, Paris, France). The synthesis and characteristics of compounds **1**−**11** (Table 1) have been published previously (*8*−*10*, *13*). Other reagents were purchased from Aldrich, Sigma, or Acros unless otherwise indicated and were of the highest purity commercially available.

*Protein Expression and Purification.* The iNOS, nNOS, and eNOS oxygenase domains (amino acids 1−498, 1−720, and 1−491, respectively) containing a six-histidine tag at their C-termini were overexpressed in *Escherichia coli* as previously described (*14*−*16*). Recombinant full-length inducible NOS was isolated and purified from *E. coli* as reported previously (*17*). NOSs were estimated to be more than 95% pure by SDS−PAGE. Protein concentrations were determined by the method of Bradford using bovine serum albumin as a standard and the Bradford reagent from Bio-Rad (*18*).

Buffers used for protein purification and storage contained DTT which forms a bisthiolate complex with NOSs. To avoid the presence of several heme species in the starting solution, proteins were filtered over a Bio-Spin column (Bio-Rad), preliminarily equilibrated with 50 mM Hepes buffer (pH 7.4), before use.

*Incorporation of $BH_4$ in Pterin-Free $iNOS_{oxy}$.* The reconstitution of $iNOS_{oxy}$ has been shown to be slow and to only occur in the presence of a reduced thiol (*19*, *20*). We routinely incorporated $BH_4$ under the following conditions. $iNOS_{oxy}$ was incubated overnight (15 h) at 4 °C in 50 mM Hepes buffer (pH 7.4), in the presence of 25 $\mu$M $BH_4$ and 1 mM DTT. Under these conditions, one observed the progressive disappearance of the bisthiolate species absorbing at 460 nm and the appearance of a high-spin species absorbing around 395 nm (data not shown; see ref *20*). This transition is usually considered a direct consequence of $BH_4$ binding (*19*, *20*). The Soret band of the resulting solution, as observed by absolute spectroscopy, was broad with a maximum absorption wavelength of ~400 nm, and a residual absorbance around 460 nm indicated that a minor fraction of the enzyme was still under a bisthiolate form, depending on the sample and on the preincubation.

*UV−Visible Studies of the Interaction of NOS with Various Compounds.* Studies were carried out at room temperature in a UVIKON 942 spectrophotometer (Kontron Biotek), in 1 cm path length cuvettes (150 $\mu$L total volume) containing 0.6−1 $\mu$M NOS or NOS oxygenase domain. Assayed compounds were dissolved in buffer and added stepwise to the sample cuvette, whereas equivalent volumes of buffer were added to the reference cuvette. Dissociation constants ($K_s$) of the NOS−ligand complexes were calculated from the plots of $1/\Delta A(\lambda_{max} - \lambda_{min})$ versus 1/[ligand] using KaleidaGraph.

*Resonance Raman Spectroscopy.* The Raman spectra were recorded at 20 ± 1 °C using a Jobin-Yvon spectrophotometer (HG 2S) with the 413.1 nm excitation of a $Kr^+$ laser (Coherent Innova). Using radiant laser powers of 15−40 mW, the RR spectra (two to eight scans) were collected, imported, checked, and analyzed with Grams/32 (Galactic Industries). Under these conditions, the frequency precision is 0.5−3 $cm^{-1}$, depending on the intensity of the bands.

*EPR Spectroscopy.* EPR spectra were recorded on a Bruker EPR Elexsys 500 spectrometer operating at X-band frequency (9.44 GHz) equipped with a shq0011 cavity fitted with an Oxford Instruments liquid helium probe. The following instrument settings were used: modulation frequency of 100 kHz, modulation amplitude of 1 mT, time constant of 0.04 s, field sweep of 400 mT, microwave power of 10 mW, sampling time of 41 ms, and two scans. Quartz tubes containing $BH_4$-free $iNOS_{oxy}$ alone (50 $\mu$L, 15 $\mu$M), or in the presence of the studied compounds, were frozen in cold ethanol and then in liquid nitrogen. All spectra were recorded at 15 and 120 K. The method of Taylor (*21*) for calculation of crystal field parameters and the following equations giving the rhombic ($V$) and axial ($\Delta$) ligand field terms in unit of spin−orbit constant $\zeta$ were used as described previously (*13*).

$$V/\zeta = g_x/(g_z + g_y) + g_y/(g_z - g_x)$$

$$\Delta/\zeta = g_x/(g_z + g_y) + g_z/(g_y - g_x) - V/2\zeta$$

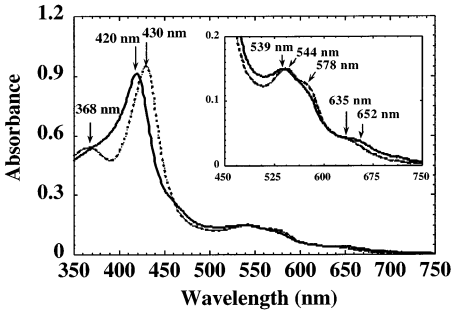


FIGURE 1: UV−visible spectra of $BH_4$-free $iNOS_{oxy}$ before (—) and after the addition of 1 mM *N*-benzyl-*N*′-hydroxyguanidine **1** (- - -). Spectra were recorded in 50 mM Hepes buffer (pH 7.4) at room temperature as described in Materials and Methods.

## RESULTS

*UV−Visible Studies of the Interaction of $BH_4$-Free $iNOS_{oxy}$ with N-Hydroxyguanidines.* The UV−visible spectrum of $BH_4$-free $iNOS_{oxy}$ expressed in *E. coli* (*14*) exhibited a Soret peak at 420 ± 2 nm (Figure 1). The position of this Soret peak indicated that its iron(III) predominantly existed in a low-spin state with a water molecule bound in the *trans* position of its cysteinate axial ligand as described previously (*14*). The resting Fe(III) state of $BH_4$-free $iNOS_{oxy}$ also exhibited a peak at 539 nm and shoulders around 578 and 652 nm.

The progressive addition of *N*-(4-*tert*-butylphenyl)-*N*′-hydroxyguanidine, **6**, to $BH_4$-free $iNOS_{oxy}$ led to the appearance of a difference spectrum characterized by a peak at 389 nm and a trough at 423 nm (Table 1). This difference spectrum, usually called a type I spectrum, is due to the binding of a substrate to the protein of NOS and cytochrome P450 in the proximity of the heme, which results in the loss of the water ligand of the low-spin ferric heme protein and formation of the corresponding pentacoordinate high-spin ferric species (*22*). This type of difference spectrum was previously obtained upon binding of NOHA to a low-spin $iNOS_{oxy}$−Fe(III) complex with formation of the pentacoordinate high-spin $iNOS_{oxy}$−Fe(III) complex (*22*) in which the *N*-hydroxyguanidine function of NOHA has an orientation almost parallel to the heme (*11*, *23*). The same type I difference spectrum was also the only one observed in the case of *N*-[4-(trifluoromethyl)phenyl]-*N*′-hydroxyguanidine **7** (Table 1).

A second type of interaction was observed after addition of all the other *N*-alkyl- or *N*-aryl-*N*′-hydroxyguanidines **1**−**5** and **8**−**11** to $BH_4$-free $iNOS_{oxy}$. This interaction was characterized by a peak at 439 ± 3 nm and a trough around 410 nm (Table 1 and Figure 2) during difference visible spectroscopy. The corresponding difference spectrum, called type II′ in the following, was the only one that appeared after addition of *N*-hydroxyguanidines **1**−**5** (Table 1). The nature of the complex leading to such type II′ spectra was then studied in a more detailed manner in the case of compound **1**.

*Spectral Studies of the Complex formed between $BH_4$-Free $iNOS_{oxy}$ and N-Benzyl-N′-hydroxyguanidine **1**.* Gradual addition of **1** to $BH_4$-free $iNOS_{oxy}$ led to the appearance of a difference spectrum characterized by a peak at 437 ± 1 nm and a broad trough centered around 400 nm (Figure 2). A dissociation constant $K_s$ of 140 ± 30 $\mu$M was calculated from

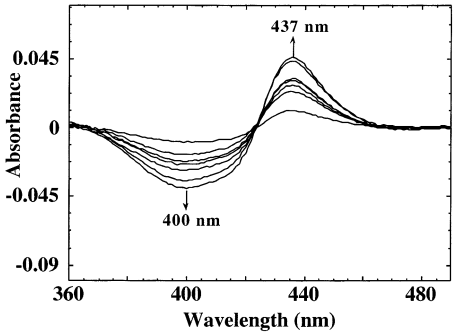


FIGURE 2: Difference spectra obtained upon addition of increasing concentrations of *N*-benzyl-*N*′-hydroxyguanidine **1** to a $BH_4$-free $iNOS_{oxy}$ solution. Spectra were recorded in 50 mM Hepes buffer (pH 7.4) as described in Materials and Methods.

the plot of $1/\Delta A(437-400$ nm) versus 1/[**1**] (Table 1). In the presence of a saturating concentration of **1**, $BH_4$-free $iNOS_{oxy}$ exhibited an absolute spectrum characterized by a Soret peak red-shifted by 10 nm when compared to that of the resting protein, and by other peaks at 368 and 544 nm and shoulders at 578 and 635 nm (Figure 1). Reduction of the iron by sodium dithionite in the presence of CO, at this stage, led to a strong Soret peak at 444 nm with only a weak shoulder at 420 nm, corresponding to the iron(II)−CO complex of the starting heme protein (data not shown). This last result indicated that the formation of the $BH_4$-free $iNOS_{oxy}$ complex with **1** does not lead to an irreversible change of the protein.

To compare the effects of **1** with that of a usual heme ligand, we performed similar spectral experiments with imidazole. The difference spectrum observed upon progressive addition of imidazole to a $BH_4$-free $iNOS_{oxy}$ solution displayed a peak at 434 nm and a trough at 396 nm. Such difference spectra, called type II spectra, are usually found for complexes of cytochrome P450 and NOS with nitrogenous ligands (*24*). The solution obtained after addition of 1 mM imidazole to $BH_4$-free $iNOS_{oxy}$ showed an absolute spectrum characterized by peaks at 360, 428, and 528 nm that are clearly blue-shifted when compared to those of the $BH_4$-free $iNOS_{oxy}$−**1** complex. Because of the similarity of the UV−visible spectra observed with imidazole and **1**, the difference spectra obtained upon addition of **1** and other *N*-hydroxyguanidines producing identical effects to $BH_4$-free $iNOS_{oxy}$ were termed type II′ difference spectra.

Interaction of **1** with $BH_4$-free $iNOS_{oxy}$ was then studied by EPR spectroscopy at 15 and 120 K. The EPR spectra of the native protein at these two temperatures showed that it existed as a mixture of a high-spin species characterized by a signal at $g = 7.61$ (observed at 15 K, data not shown) and a major low-spin species characterized by *g* signals at 1.94, 2.25, and 2.35 (Figure 3a) (*25*). Addition of 1 mM **1** led to the disappearance of the high-spin signal at $g = 7.61$ and the appearance of a new low-spin species characterized by *g* values at 1.93, 2.24, and 2.38 that only slightly differ from those of starting low-spin $BH_4$-free $iNOS_{oxy}$. However, they correspond to a different low-spin species as shown by the coexistence of the two sets of signals after the addition of 1 mM **1** (Figure 3b). Upon addition of 12 mM **1**, the signals of the starting low-spin $BH_4$-free $iNOS_{oxy}$ completely disappeared, and the spectrum only corresponded to the species characterized by peaks at 1.93, 2.24, and 2.38 (Figure 3c).

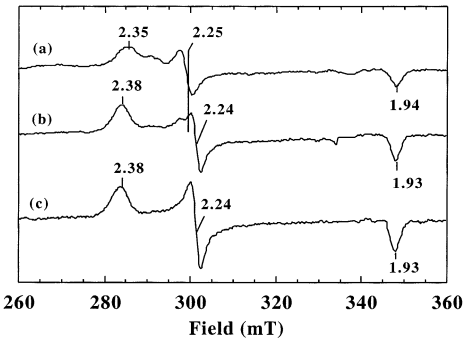


FIGURE 3: X-Band EPR spectra at 120 K of 15 $\mu$M $BH_4$-free $iNOS_{oxy}$ before (a) and after the addition of 1 mM (b) and 12 mM *N*-benzyl-*N*′-hydroxyguanidine **1** (c). $BH_4$-free $iNOS_{oxy}$ and compound **1** were mixed at room temperature in 50 mM Hepes buffer (pH 7.4), placed in an EPR tube, and cooled at 120 K before the spectra were recorded under the conditions described in Materials and Methods.

Table 2: EPR Data for Several Heme Fe(III) Low-Spin Complexes[a]

| complex | *g* values | $\Delta/\zeta$, $V/\Delta$ | ref |
|---|---|---|---|
| $BH_4$-free $iNOS_{oxy}$−**1** | 1.93, 2.24, 2.38 | 6.8, 0.40 | this work |
| $BH_4$-free $iNOS_{oxy}$−ImH | 1.87, 2.30, 2.49 | 5.1, 0.40 | this work |
| $BH_4$-free $iNO_{oxy}$−DTT | 1.93, 2.25, 2.37 | 6.7, 0.33 | this work |
| MP-8 Fe(III)−**3** | 1.86, 2.26, 2.55 | 5.2, 0.59 | *13* |
| MP-8 Fe(III)−ImH | 1.49, 2.26, 2.98 | 3.0, 0.79 | *13* |

[a] $\Delta/\zeta$ is the tetragonal field expressed in units of spin−orbit coupling constant $\zeta$, and $V/\Delta$ is the rhombicity. Crystal field parameters were calculated with the convention originally used by Peisach and Blumberg (*39*), i.e., $g_y > -g_x > -g_z > 0$.

For the sake of comparison, similar experiments were performed with two usual iron ligands of NOS, imidazole and DTT. Addition of 1 mM imidazole or 9 mM DTT to $BH_4$-free $iNOS_{oxy}$ also led to the disappearance of the high-spin signal of the native protein and the appearance of new low-spin complexes characterized by the *g* values indicated in Table 2. Interestingly, the EPR characteristics (*g* values and tetragonal field $\Delta/\zeta$) of the complexes of $BH_4$-free $iNOS_{oxy}$ with **1** and DTT were very similar (Table 2).

The complex between $BH_4$-free $iNOS_{oxy}$ and **1** was also studied by resonance Raman spectroscopy. The high-frequency region (1300−1700 $cm^{-1}$) of the RR spectrum of this complex was indicative of a hexacoordinate low-spin heme−Fe(III) state (Table 3). The oxidation state marker band $\nu_4$ and the spin sensitive mode $\nu_3$ were observed at 1374 and 1502 $cm^{-1}$, respectively, as expected for a low-spin heme−Fe(III) species (*26*, *27*). In fact, those bands were at the same positions in the RR spectrum of native $BH_4$-free $iNOS_{oxy}$ which is predominantly low-spin, and in the spectrum of the previously described low-spin iron(III) complexes, nNOS Fe(III)−imidazole, and the low-spin fraction of native eNOS Fe(III) (Table 3) (*28*, *29*). On the contrary, the high-spin fraction of native eNOS Fe(III) exhibits a $\nu_3$ band at a very different position (1489 $cm^{-1}$) (*30*). Moreover, the RR spectrum of the $BH_4$-free $iNOS_{oxy}$−**1** complex did not show any signal corresponding to an iron(II) species that could have been derived from a reduction of $BH_4$-free $iNOS_{oxy}$ by **1**, and that should have led to a $\nu_4$ band in the 1345 $cm^{-1}$ region (*26*). Finally, the only major change observed in the low-frequency region (350−750 $cm^{-1}$) of the RR spectrum of $BH_4$-free $iNOS_{oxy}$ upon addition of 10 mM **1** was a shift from 377 to 371 $cm^{-1}$ of the band

Table 3: Comparison of the High-Frequency RR Modes ($cm^{-1}$) of Various NOS Complexes

| complex | $\nu_4$ | $\nu_3$ | $\nu_2$ region | $\nu_{10}$ |
|---|---|---|---|---|
| $BH_4$-free $iNOS_{oxy}$ | 1374 | **1503** | 1561−1576 | 1629−1637 |
| $BH_4$-free $iNOS_{oxy}$−**1**[a] | 1374 | **1502** | 1560−1575 | 1626−1636 |
| $BH_4$-containing $nNOS_{oxy}$ Fe(III)−ImH (6 mM) [b] | 1372 | **1501** | 1577 | 1634 |
| $BH_4$-containing nNOS Fe(II) [c] | 1347−1360 | **1466** | 1553−1584 | 1600−1617 |
| $BH_4$-containing native eNOS Fe(III) (high-spin fraction)[d] | 1370 | **1489** | 1563 | nd[e] |
| $BH_4$-containing native eNOS Fe(III) (low-spin fraction)[d] | 1374 | **1503** | 1579 | 1638 |

[a] RR spectrum of 25 $\mu$M $BH_4$-free $iNOS_{oxy}$ Fe(III) in the presence of 10 mM **1** (see Materials and Methods). The excitation wavelength was 413.1 nm. [b] From ref *28*. [c] From ref *29*. [d] From ref *30*. [e] Not determined.

corresponding to a deformation mode of the heme propionates (*30*, *31*).

*Effect of the Nature of the N-Aryl (or N-Alkyl) Substituent on the Type of Complex Formed between N-Aryl (or N-Alkyl) N′-Hydroxyguanidines and $BH_4$-Free $iNOS_{oxy}$.* Table 1 compares the types of difference spectra and the $K_s$ values observed for the complexes formed with 11 N-substituted *N*′-hydroxyguanidines. All those bearing an *N*-alkyl substituent (**1**, **4**, **10**, and **11**) mainly led to type II′ complexes that are characterized by a peak around 438 nm. *N*-Hydroxyguanidine, **5**, only led to a type II′ spectrum. The situation is more complex with *N*-aryl-*N*′-hydroxyguanidines, as **2** and **3** exclusively led to a type II′ spectrum whereas **6** and **7** only gave a type I spectrum, and **8** and **9** led to a mixture of type I and II′ spectra.

For all the compounds producing a single type of spectrum, plots of $1/\Delta A(\lambda_{max} - \lambda_{min}) = f(1/[\text{ligand}])$ could satisfactorily be fitted with a linear function, leading to the $K_s$ values listed in Table 1. For the compounds producing a mixture of type I and type II′ difference spectra, only a rough estimation of the $K_s$ value could be made on the basis of the ligand concentration responsible for half the maximum $\Delta A$ value. *N*-Hydroxyguanidine, **5**, exhibited the lowest affinity with a $K_s$ value of ~4 mM, and in a general manner, the compounds not bearing an aryl substituent, such as **4**, **10**, and **11**, showed $K_s$ values at the millimolar level. *N*-Aryl-*N*′-hydroxyguanidines exhibited better affinities with $K_s$ values between 200 and 400 $\mu$M, irrespective of the type of spectrum observed. Finally, the compound that led to the highest affinity ($K_s$ = 140 $\mu$M) and the maximum amplitude of the corresponding difference spectrum was *N*-benzyl-*N*′-hydroxyguanidine, **1**.

The absolute UV−visible spectra observed after addition of saturating amounts of the *N*-hydroxyguanidines to $BH_4$-free $iNOS_{oxy}$ exhibited a Soret peak either red-shifted (from 420 to 430 nm) when compared to that of the native protein for the compounds producing a type II′ difference spectrum (**1**−**5** and **9**−**11**) or blue-shifted (from 400 to 397 nm) for those producing a type I difference spectrum (Table 1).

Table 4 shows the effect of pH on the interaction between $BH_4$-free $iNOS_{oxy}$ and the compounds leading to the most important type II′ and type I difference spectra (**1** and **7**, respectively). An increase in the pH of the solution from 6.9 to 8.0 led to a marked decrease in the $K_s$ value found for compound **1** (from 150 to 37 $\mu$M), without significant changes in the type and intensity of the difference spectrum. On the other hand, this pH increase led to an important increase in the $K_s$ value measured for compound **7**, which always gave a type I difference spectrum.

*Effects of the Presence of $BH_4$ on the Interaction between $iNOS_{oxy}$ and Compounds **1**−**11**.* $BH_4$ has been shown to have dramatic effects on the topology of the distal heme binding pocket, with important consequences on the coordination properties of the iron toward typical heme ligands, such as CO (*32*) and nitrosoalkanes (*33*), or upon reaction with aryldiazenes (*34*). We thus compared the interactions of compounds **1**−**11** with $iNOS_{oxy}$ containing $BH_4$.

Table 4: Effects of pH on the Characteristics of the Visible Difference Spectra Obtained upon Addition of **1** and **7** to $BH_4$-Free $iNOS_{oxy}$[a]

| | spectral characteristics | | |
|---|---|---|---|
| ligand | pH 6.9 | pH 7.4 | pH 8.0 |
| **1** | type II′ $K_s = 150 \pm 30$ $\mu$M | type II′ $K_s = 140 \pm 30$ $\mu$M | type II′ $K_s = 37 \pm 19$ $\mu$M |
| **7** | type I $K_s = 366 \pm 42$ $\mu$M | type I $K_s = 420 \pm 160$ $\mu$M | type I $K_s = 820 \pm 200$ $\mu$M |

[a] Type I and II′ spectra are defined as in Table 1. No significant difference in $\lambda_{max}$ and $\lambda_{min}$ values was observed at the different pH values. Means ± the standard deviation from at least three experiments.

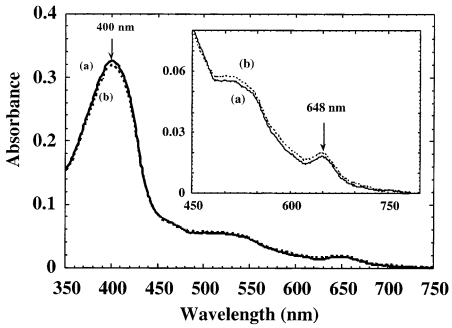


FIGURE 4: UV−visible spectra of $BH_4$-free $iNOS_{oxy}$ preincubated overnight at 4 °C with 25 $\mu$M $BH_4$ and 1 mM DTT before (—) and after the addition of 1 mM *N*-benzyl-*N*′-hydroxyguanidine **1** (- - -). Spectra were recorded in 50 mM Hepes buffer (pH 7.4) at room temperature as described in Materials and Methods.

Reconstitution of the protein with $BH_4$ was performed, as described recently (*19*, *20*), by coincubation of 1 $\mu$M $BH_4$-free $iNOS_{oxy}$ with 25 $\mu$M $BH_4$ and 1 mM DTT, for 14 h at 4 °C. The resulting protein displayed a Soret peak at 400 ± 2 nm, indicating that, in agreement with previous literature data (*20*), incorporation of $BH_4$ has led to a marked increase in the level of the high-spin pentacoordinate state of $iNOS_{oxy}$. Addition of 5 mM **1** to $BH_4$-containing $iNOS_{oxy}$ did not result in any significant change in the absolute UV−visible spectrum of the protein (Figure 4). In a similar manner, all the compounds that produced type II′ spectra when added to $BH_4$-free $iNOS_{oxy}$ (**1**−**5** and **9**−**11**) failed to produce any red shift of the Soret peak of $BH_4$-contaning $iNOS_{oxy}$ (data not shown).

Control experiments were performed by preincubating $BH_4$-free $iNOS_{oxy}$ under the reconstitution conditions (pres-

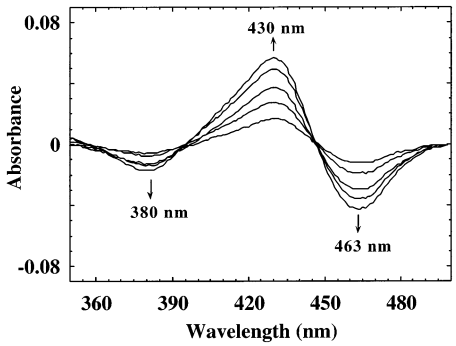


FIGURE 5: Difference spectra obtained upon addition of increasing concentrations of *N*-benzyl-*N*′-hydroxyguanidine **1** to a solution of $BH_4$-free $iNOS_{oxy}$ after partial incorporation of $BH_4$. $BH_4$-free $iNOS_{oxy}$ was preincubated for 2 h at 4 °C in the presence of 25 $\mu$M $BH_4$ and 1 mM DTT, and spectra were recorded in 50 mM Hepes buffer (pH 7.4) at room temperature as described in Materials and Methods.

ence of 1 mM DTT) but in the absence of $BH_4$. As expected, the resulting protein was mainly under the form of a hexacoordinate bisthiolate complex exhibiting a split Soret peak at 385 and 460 nm (*35*). Addition of 1 mM **1** to that complex led to a difference spectrum characterized by a peak at 432 nm and troughs at 464 and 388 nm. Moreover, the absolute UV−visible spectrum of the solution exhibited a Soret peak at 430 nm, as the complex derived from **1** and $BH_4$-free $iNOS_{oxy}$ in the absence of DTT (Table 1). These data show that DTT alone does not inhibit the formation of the type II′ complex between $BH_4$-free $iNOS_{oxy}$ and **1**.

In another set of experiments, $BH_4$-free $iNOS_{oxy}$ was anaerobically preincubated with 50 $\mu$M $BH_4$ and 5 mM GSH at 20 °C for 2 h. The Soret peak of the resulting protein was found at 400 ± 2 nm. As in the experiment shown in Figure 4, addition of 10 mM **1** did not lead to any change in the visible spectrum of the solution (data not shown). These data showed that the inhibitory effects of preincubation of $BH_4$-free $iNOS_{oxy}$ with $BH_4$ and a thiol on the formation of a low-spin complex with **1** did not depend on the nature of the thiol that was used.

Finally, interaction of **1** was studied with a solution of $iNOS_{oxy}$ partially reconstituted with $BH_4$ which was obtained after incubation for only 2 h with 25 $\mu$M $BH_4$ and 1 mM DTT. As expected, the visible spectrum of this protein exhibited a peak at 402 nm and a shoulder at 460 nm, indicating that the protein was under the form of a pentacoordinate high-spin species as well as of a hexacoordinate bisthiolate complex (data not shown). Progressive addition of compound **1** led to a difference spectrum showing a peak at 430 nm and troughs at 463 and 380 nm (Figure 5), which was very similar to that described above with the protein preincubated with DTT but without $BH_4$. This indicated that the species interacting with **1** was the fraction of the protein that did not contain $BH_4$ and existed as an iron(III)−bisthiolate complex. Accordingly, the absolute spectrum of the solution exhibited a broad Soret peak around 402 nm, which showed that the major fraction of the protein having bound $BH_4$ had not reacted with **1**.

All these data clearly showed that, unlike $BH_4$-free $iNOS_{oxy}$, $BH_4$-repleted $iNOS_{oxy}$ did not interact with compound **1** to form a low-spin type II′ complex.

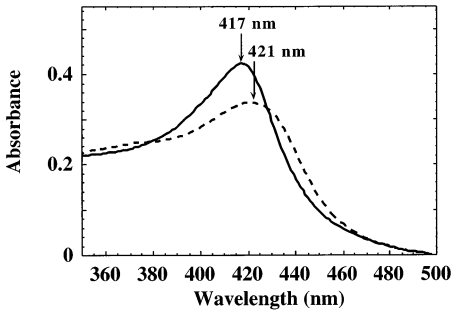


FIGURE 6: Absolute visible spectra (Soret region) of $BH_4$-free $nNOS_{oxy}$ in the absence (—) and in the presence of 1 mM *N*-benzyl-*N*′-hydroxyguanidine **1** (- - -). Conditions were those described in the legend of Figure 1.

*Interaction between **1** and $BH_4$-Free Full-Length iNOS, $BH_4$-Free $nNOS_{oxy}$, or $BH_4$-Free $eNOS_{oxy}$.* $BH_4$-free full-length iNOS contains the iNOS reductase domain and was obtained by expression in *E. coli* (*17*). Its visible spectrum exhibited a Soret peak at 420 nm, indicating that it mainly existed under a low-spin Fe(III) state. Upon addition of compound **1**, its Soret peak was shifted to 430 nm (data not shown), in a manner identical to that observed in experiments performed with $BH_4$-free $iNOS_{oxy}$ (Figure 1). Thus, the presence of the NOS reductase domain does not inhibit the formation of type II′ complexes between the $BH_4$-free iNOS oxygenase domain and *N*-hydroxyguanidines such as **1**.

Similar experiments have then been carried out with recombinant $BH_4$-free oxygenase domains of nNOS and eNOS. Native $BH_4$-free $nNOS_{oxy}$ displayed a wide Soret band around 417 nm (Figure 6), indicating that it mainly existed under a low-spin ferric state, but with a larger fraction of the protein under a high-spin form when compared to $BH_4$-free $iNOS_{oxy}$ (compare Figures 1 and 6). Addition of compound **1** led to a type II′ difference spectrum characterized by a peak at 432 nm. However, even with 5 mM **1**, this difference spectrum was much less intense than the one observed with $BH_4$-free $iNOS_{oxy}$ under identical conditions (data not shown). These data were in complete agreement with the absolute visible spectrum of $BH_4$-free $nNOS_{oxy}$ in the presence of 5 mM **1** which showed a wide Soret band at 421 nm (Figure 6), much less red-shifted than that formed in the case of $BH_4$-free $iNOS_{oxy}$ (Figure 1). In a more general manner, all the *N*-hydroxyguanidines that produced a type II′ spectrum with $BH_4$-free $iNOS_{oxy}$ (**1**−**5** and **8**−**11**) also led to such an interaction with $BH_4$-free $nNOS_{oxy}$, however with a much lower intensity, as shown by the smaller red shift of the Soret peaks observed in the corresponding absolute spectra (Table 5) (maximum red shift of 4 nm, instead of 10 nm in the case of $BH_4$-free $iNOS_{oxy}$). Interestingly, compounds **6** and **7** that led to a type I interaction with $BH_4$-free $iNOS_{oxy}$ also led to such an interaction with $BH_4$-free $nNOS_{oxy}$.

Finally, comparative experiments were carried out with recombinant $BH_4$-free $eNOS_{oxy}$. The native protein exhibited a Soret peak around 406 nm, indicating that it mainly existed under a high-spin form, unlike $BH_4$-free $iNOS_{oxy}$ and $BH_4$-free $nNOS_{oxy}$. Addition of **1** or all the *N*-hydroxyguanidines that formed type II′ complexes with $BH_4$-free $iNOS_{oxy}$ and

Table 5: Characteristics of the Visible Spectra Obtained upon Interaction of $BH_4$-Free $nNOS_{oxy}$ with Several *N*-Hydroxyguanidines, R−NH−C(=NOH)−$NH_2$, at pH 7.4

| ligand | R | difference spectrum type[a] | absolute spectrum $\lambda_{sat}$[b] (nm) |
|---|---|---|---|
| **1** | $C_6H_5-CH_2$ | II′ | 421 |
| **2** | 4-HO−$C_6H_4$ | II′ | 421 |
| **3** | 4-$CH_3O-C_6H_4$ | II′ | 420 |
| **4** | *n*-$C_5H_{11}$ | I and II′ | 418 |
| **5** | H | II′ | 421 |
| **6** | 4-tBu−$C_6H_4$ | I | 397 |
| **7** | 4-$CF_3-C_6H_4$ | I | 410 |
| **8** | 4-Cl−$C_6H_4$ | II′ | 420 |
| **9** | 4-$CH_3-C_6H_4$ | II′ | 420 |
| **10** | *n*-$C_4H_9$ | II′ | 421 |
| **11** | *n*-$C_6H_{13}$ | II′ | 419 |

[a] Type I and II′ difference spectra are defined as in Table 1. [b] $\lambda_{sat}$ is the position of the Soret peak of the absolute spectrum of the enzyme after addition of 4 mM ligand, except in the case of **5** and **10**, for which a concentration of 12 mM was used.

$nNOS_{oxy}$ to $BH_4$-free $eNOS_{oxy}$ completely failed to induce a red shift of its Soret peak.

## DISCUSSION

Our study of the interaction of many *N*-alkyl- and *N*-aryl-*N*′-hydroxyguanidines with NOS shows that these compounds have two possible binding modes in the NOS active site. The first one is usual for such heme−cysteinate proteins and corresponds to a binding to the protein in the proximity of the heme that leads to a transition from hexacoordinate low-spin NOS Fe(III) to pentacoordinate high-spin NOS Fe(III) characterized by a type I difference spectrum (*22*). The second one has never been described so far in the case of NOS. It corresponds to the binding of the *N*-hydroxyguanidine to the NOS iron with the formation of a new low-spin Fe(III) complex, as shown by UV−visible, EPR, and RR spectroscopy (Figures 1−3).

*Nature of the $BH_4$-Free iNOS Iron−N-Hydroxyguanidine Complexes.* The formation of similar Fe(III)−*N*-hydroxyguanidine complexes has recently been reported upon addition of *N*-alkyl- and *N*-aryl-*N*′-hydroxyguanidines to microperoxidase-8 (MP-8), a small heme protein, derived from proteolytic cleavage of cytochrome *c*, whose iron axial ligand is a histidine (*13*). $BH_4$-free iNOS exhibits a behavior similar to that of the MP-8−Fe(III) complex toward compounds containing a C=N−OH function, as it forms low-spin Fe(III) complexes with *N*-hydroxyguanidines (Table 1), but not with aldoximes or ketoximes such as *p*-methoxybenzaldoxime or *p*-methoxyacetophenone oxime (data not shown).

A priori, compounds involving a C=N−OH function may bind to iron porphyrin complexes either via their oxygen atom or via their nitrogen atom. N binding of *N*-hydroxyguanidines to heme complexes seems to be less likely for the two following reasons. Recent studies about the N binding of compounds involving a C=N−OH moiety to iron(II) porphyrins and cytochromes P450 Fe(II) have shown that this binding is greatly dependent on the steric hindrance that exists between the heme plane and the C substituents of the C=NOH function (*36*, *37*). Thus, from all the C=NOH compounds that have been tested, only *Z*-aldoximes were found to be able to bind to heme iron(II) via their nitrogen atom. This shows that N binding is only possible for compounds having a hydrogen atom as a very small C substituent closest to the heme. Such severe steric problems should greatly disfavor N binding of compounds involving a C=NOH moiety to iron porphyrins. The second argument against N binding of *N*-hydroxyguanidines to $BH_4$-free NOS or MP-8 Fe(III) is the lack of complex formation with *N*-aryl-*N*′-methoxyguanidines, whereas the corresponding *N*-aryl-*N*′-hydroxyguanidines lead to the low-spin type II′ complexes described in this paper. This has been already reported in the case of MP-8 (*13*), and we found that this was also true for $BH_4$-free $iNOS_{oxy}$. Thus, *N*-*p*-methoxyphenyl-*N*′-methoxyguanidine was unable to form a new type II′ complex with $BH_4$-free $iNOS_{oxy}$ (data not shown), unlike *N*-*p*-methoxyphenyl-*N*′-hydroxyguanidine **3** (Table 1). If *N*-hydroxyguanidines were N-bonded to $BH_4$-free NOS or MP-8 Fe(III), one would not expect that replacement of their N−OH moiety with an N−$OCH_3$ group would prevent complex formation.

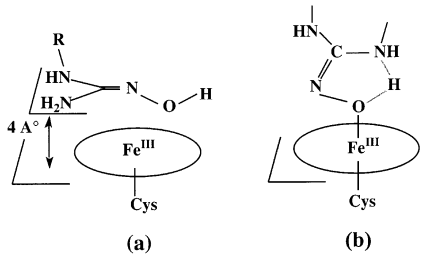


FIGURE 7: Schematic structures of the two types of complexes formed between $BH_4$-free NOS and *N*-hydroxyguanidines. (a) Type I binding mode, analogous to the one observed in the X-ray structure of the $iNOS_{oxy}$−NOHA complex (*11*). (b) Type II′ binding mode with *N*-hydroxyguanidine acting as an iron ligand, as previously found in MP-8−*N*-hydroxyguanidine complexes (*13*). The binding mode shown in panel b is similar to that found for a complex between fluorenone oxime and an iron(III) porphyrin (*38*).

The requirement of the presence of an (N)−OH function (but not of an N−$OCH_3$ function) for the formation of type II′ complexes of $BH_4$-free NOS and MP-8 Fe(III) is easily understandable if one admits that O binding occurs after deprotonation (or weakening via hydrogen bonding) of the O−H bond (Figure 7b). Such an O binding mode of the deprotonated form of a C=NOH compound has recently been described in a porphyrin Fe(III) complex with fluorenone oxime (*38*). The spectral characteristics of the MP-8 Fe(III)−*N*-hydroxyguanidine complexes, and particularly their EPR data, have led us to propose that *N*-hydroxyguanidines bind to MP-8 Fe(III) via their oxygen atom after deprotonation or weakening of their (N)O−H bond (*13*). Table 2 compares the EPR data obtained for the complexes of $BH_4$-free $iNOS_{oxy}$ with **1** and with two usual NOS Fe(III) ligands, imidazole and DTT, and for the complexes of MP-8 with the *N*-hydroxyguanidine **3** and with imidazole. Analysis of the EPR data of these complexes has been carried out according to Taylor's equations that are widely used for assigning the ligands of not completely characterized low-spin heme Fe(III) complexes (*21*, *39*). The tetragonal field values, $\Delta/\zeta$, found for the $BH_4$-free $iNOS_{oxy}$ complexes with **1** and imidazole (6.8 and 5.1, respectively) are much larger than those observed for the corresponding MP-8 complexes (5.2 and 3.0, respectively). These data indicate that the proximal

cysteinate ligand of $BH_4$-free $iNOS_{oxy}$ is still present after-coordination of **1**, as it is known that the cysteinate ligand is responsible for a strong axial distortion of the heme iron, leading to high $\Delta/\zeta$ values, in all heme−thiolate ferric complexes (*40*, *41*). The much higher $\Delta/\zeta$ value observed for the MP-8 complex with **3**, when compared to that of the MP-8−imidazole complex, was described as indirect evidence for the coordination of **3** via an especially electron-rich oxygen atom (after deprotonation or weakening of the O−H bond of **3**) (*13*). Interestingly, the $BH_4$-free $iNOS_{oxy}$ complex with **1** also exhibits a $\Delta/\zeta$ value much higher than the one found for the $BH_4$-free $iNOS_{oxy}$−imidazole complex (6.8 instead of 5.1). This led us to propose a similar mode of binding of the oxygen atom of *N*-hydroxyguanidines to heme iron(III) in $BH_4$-free $iNOS_{oxy}$ (Figure 7b) and MP-8. Accordingly, the $\Delta/\zeta$ values observed for the $BH_4$-free $iNOS_{oxy}$ complexes with **1** and with DTT, which provides an anionic electron-rich thiolate ligand, are almost identical.

All these data are in favor of the O binding of *N*-hydroxyguanidines to MP-8 Fe(III) and $BH_4$-free iNOS Fe(III); however, supplementary experiments are required before definite conclusions about this binding mode can be made.

Finally, the conclusion that *N*-hydroxyguanidines bind in a manner very similar to that of MP-8 and $BH_4$-free $iNOS_{oxy}$ is in agreement with the same kind of pH dependence of the $K_s$ values that were found for these heme protein−*N*-hydroxyguanidine complexes, with a decrease in $K_s$ with an increase in pH (Table 3 and ref *13*), as expected if a deprotonated form of *N*-hydroxyguanidines is involved in iron complex formation (*13*). On the contrary, increasing the pH leads to an important increase in the $K_s$ values measured for $BH_4$-free $iNOS_{oxy}$ complexes with *N*-hydroxyguanidines that give type I difference spectra such as **7** (Table 4). This result is expected as these type I complexes involve the binding of *N*-hydroxyguanidines to the protein, in the proximity of the heme, with a major interaction between a glutamate residue of the protein with the *N*-hydroxyguanidine moiety, which should be favored if the *N*-hydroxyguanidine is protonated.

*Factors Determining the Mode of Binding of N-Hydroxyguanidines to NOS.* First of all, it is noteworthy that the binding mode involving an iron−*N*-hydroxyguanidine bond was so far observed with only $BH_4$-free NOS. Thus, the presence of $BH_4$ and its influence on the structure of the distal part of the NOS heme pocket have dramatic inhibitory effects on the formation of iron−*N*-hydroxyguanidine complexes. Inhibition of the formation of NOS Fe(II) complexes with nitrosoalkanes (*33*) and of NOS Fe(III) complexes with thiolate ligands such as DTT (*14*, *35*), in the presence of $BH_4$, has been previously reported.

On the contrary, the presence of the reductase domain of $BH_4$-free iNOS does not inhibit the formation of such complexes (above data comparing interactions of **1** with $BH_4$-free $iNOS_{oxy}$ and $BH_4$-free iNOS). $BH_4$-free $iNOS_{oxy}$ leads to a more important formation of iron−*N*-hydroxyguanidine complexes than $BH_4$-free $nNOS_{oxy}$ (compare Tables 1 and 5), whereas $BH_4$-free $eNOS_{oxy}$ was unable to form such complexes under the conditions that were used. In fact, the amount of complex formed seems to be related to the initial amount of $BH_4$-free NOS in the low-spin state.

The structure of the *N*-alkyl (or *N*-aryl) substituent of the *N*-hydroxyguanidines has a great influence on their mode of binding to NOS, as small changes in the structure of the substituent induce a shift from one kind of binding mode to the second one (Table 1). Thus, compound **3** bearing a *p*-methoxyphenyl group only leads to a type II′ complex, whereas compound **6** bearing a *p-tert*-butylphenyl substituent exclusively leads to a type I complex. In the case of MP-8, which, unlike NOS, does not involve any distal protein pocket, it was found that stronger iron−ligand interactions were obtained with electron-rich *N*-hydroxyguanidines. This appears to be globally true with $BH_4$-free $iNOS_{oxy}$ as *N*-alkyl-*N*′-hydroxyguanidines **1**, **4**, **10**, and **11** and *N*-aryl-*N*′-hydroxyguanidines bearing electron-donating substituents on their aryl ring (**2**, **3**, and **9**) lead to an exclusive or major formation of type II′ complexes. On the contrary, compounds **7** and **8**, which bear an electron-withdrawing substituent, lead to an exclusive or major formation of type I complexes (Table 1). However, the electron richness of the *N*-hydroxyguanidine moiety does not seem to be the only factor determining the type of complex formed, as compound **6** that bears an electron-donating substituent on its aryl ring exclusively leads to a type I complex. Steric factors and/or interactions of the aryl (or alkyl) substituents with the distal part of the protein could play an important role in the choice of the preferred mode of binding to $BH_4$-free NOS. In that regard, it is noteworthy that the $K_s$ values determined for the $BH_4$-free $iNOS_{oxy}$ complexes were always lower for *N*-hydroxyguanidines bearing an aryl group ($K_s$ between 140 and 420 $\mu$M) than for those not bearing such an aryl group ($K_s$ between 1000 and 3900 $\mu$M) (Table 1). This result could be due to favorable $\pi-\pi$ interactions of these aryl substituents with aromatic amino acid residues of the protein.

A very recently described result for the intermediates formed during the catalytic cycle of L-arginine oxidation by NOS (*42*) may be discussed in relation to the possible formation of NOS iron−*N*-hydroxyguanidine complexes. Freeze−quench EPR studies of the intermediates formed upon reaction at 165 K of the one-electron-reduced eNOS Fe(II)−$O_2$ complex with L-arginine in the presence of a catalytically noncompetent $BH_4$ analogue have indicated the appearance of two low-spin Fe(III) complexes after hydroxylation of the substrate, which are characterized by EPR *g* values at 2.59, 2.25, and 1.84 and 2.54, 2.25, and 1.86. These signals have been tentatively assigned to ferri−NOS complexes in which the NOHA product is bound in a nonequilibrium conformation with its hydroxyl group coordinated to the ferric ion. At 230 K, these signals disappear; it has been proposed that this was due to the release of the coordinated hydroxyl of NOHA by the heme iron, as NOHA assumes its equilibrium conformation in which the hydroxyguanidine group of NOHA is not coordinated to the now pentacoordinated Fe(III) (*42*). In fact, the product state intermediate low-spin Fe(III) complexes observed at 165 K exhibit EPR characteristics similar to those reported for the complexes of MP-8 with **4** and of $BH_4$-free $iNOS_{oxy}$ with **1**.[2] All these data suggest that the intermediates of $BH_4$-containing NOS observed at 165 K exhibit a bond between

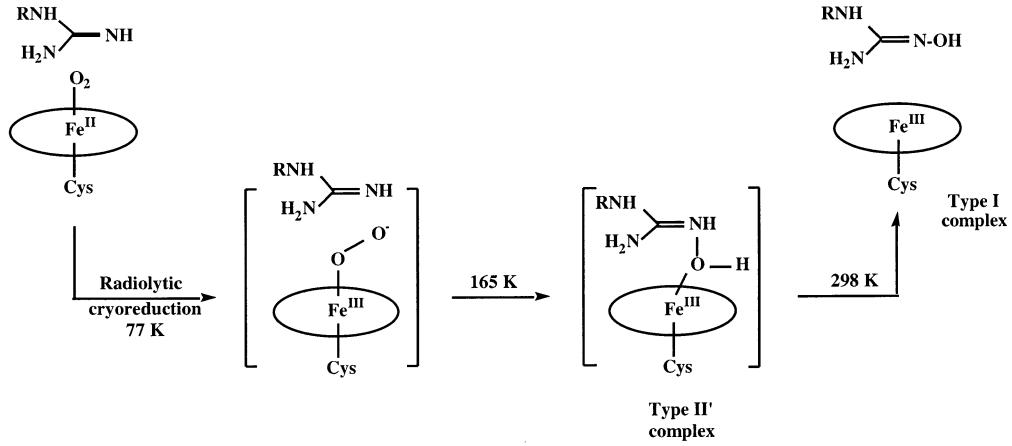


FIGURE 8: Possible intermediate formation of a type II′ NOS Fe(III)−NOHA complex upon conversion at 165 K of the active peroxo-ferri NOS−L-arginine complex, generated by radiolytic cryoreduction of NOS Fe(II)−$O_2$−L-arginine complex at 77 K, to a product state intermediate (proposition based on the results of ref *42* and of this paper).

the hydroxyguanidino oxygen atom and iron(III) similar to that of the aforementioned $BH_4$-free NOS Fe(III)−*N*-hydroxyguanidine type II′ complexes (Figure 7b). Above 230 K, these nonequilibrium product complexes would convert (Figure 8) to an equilibrium product complex of NOS containing pentacoordinated iron(III) and NOHA bound to the protein but not to the iron (type I complex, Figure 7a). The results described in this paper show that, in the presence of $BH_4$, the preferred, lowest-energy state for a NOS Fe(III)−*N*-hydroxyguanidine complex is a type I complex with the *N*-hydroxyguanidine moiety stacked over the heme ring without any iron−*N*-hydroxyguanidine bond (Figure 7a). The appearance of low-spin $BH_4$-containing NOS Fe(III)−*N*-hydroxyguanidine complexes would thus be only possible in the high-energy state generated just after irradiation of the NOS Fe(II)−$O_2$ complex, and should be transient. At the opposite end, the preferred, lowest-energy state for the $BH_4$-free Fe(III)−*N*-hydroxyguanidine complex is a type II′ complex involving an iron−*N*-hydroxyguanidine bond (Figure 7b). Further experiments are required to prove the existence of transient NOS Fe(III)−NOHA (or other *N*-hydroxyguanidines) coordination complexes in the catalytic cycle of NOS.

The results described in this paper further illustrate the ability of *N*-hydroxyguanidines to act as heme Fe(III) ligands as previously established in the case of microperoxidase MP-8 (*13*). The similar behavior of *N*-hydroxyguanidines as ligands of MP-8 and $BH_4$-free NOS suggests that these compounds could constitute a new class of good ligands of heme proteins.

## ACKNOWLEDGMENT

We thank A. Meade and J. McDonald (Cleveland Clinic Fundation) for purification of $iNOS_{oxy}$ and $nNOS_{oxy}$.

[2] One may not expect identical *g* values for the $BH_4$-free $iNOS_{oxy}$ iron(III)−**1** complex and the transient $eNOS_{oxy}$ iron(III)−L-arginine product complexes described in ref *42*, as (i) these complexes involve two different NOS domains (iNOS and eNOS), (ii) the former does not contain $BH_4$ unlike the latter, and (iii) the latter was generated under high-energy nonequilibrium conditions unlike the former.

## REFERENCES

1. Kerwin, J. F., Jr., Lancaster, J. R., Jr., and Feldman, P. L. (1995) *J. Med. Chem. 38*, 4343−4362.
2. Alderton, W. K., Cooper, C. E., and Knowles, R. G. (2001) *Biochem. J. 357*, 593−615.
3. Masters, B. S. S., McMillan, K., Sheta, E. A., Nishimura, J. S., Roman, L. J., and Martasek, P. (1996) *FASEB J. 10*, 552−558.
4. Stuehr, D. J., Kwon, N. S., Nathan, C. F., Griffith, O. W., Feldman, P. L., and Wiseman, J. (1991) *J. Biol. Chem. 266*, 6259−6263.
5. Klatt, P., Schmidt, K., Uray, G., and Mayer, B. (1993) *J. Biol. Chem. 268*, 14781−14787.
6. Crane, B. R., Arvai, A. S., Ghosh, D. K., Wu, C., Getzoff, E. D., Stuehr, D. J., and Tainer, J. A. (1998) *Science 279*, 2121−2126.
7. Raman, C. S., Li, H., Martasek, P., Kral, V., Masters, B. S. S., and Poulos, T. L. (1998) *Cell 95*, 939−950.
8. Renodon-Corniere, A., Boucher, J.-L., Dijols, S., Stuehr, D. J., and Mansuy, D. (1999) *Biochemistry 38*, 4663−4668.
9. Dijols, S., Perollier, C., Lefèvre-Groboillot, D., Pethe, S., Attias, R., Boucher, J.-L., Stuehr, D. J., and Mansuy, D. (2001) *J. Med. Chem. 44*, 3199−3202.
10. Renodon-Corniere, A., Dijols, S., Perollier, C., Lefèvre-Groboillot, D., Boucher, J.-L., Attias, R., Sari, M.-A., Stuehr, D., and Mansuy, D. (2002) *J. Med. Chem. 45*, 944−954.
11. Crane, B. R., Arvai, A. S., Ghosh, S., Getzoff, E. D., Stuehr, D. J., and Tainer, J. A. (2000) *Biochemistry 39*, 4608−4621.
12. Raman, C. S., Li, H., Martasek, P., Southan, G., Masters, B. S. S., and Poulos, T. L. (2001) *Biochemistry 40*, 13448−13455.
13. Lefèvre-Groboillot, D., Dijols, S., Boucher, J.-L., Mahy, J.-P., Ricoux, R., Desbois, A., Zimmermann, J.-L., and Mansuy, D. (2001) *Biochemistry 40*, 9909−9917.
14. Ghosh, D. K., Wu, C., Pitters, E., Moloney, M., Werner, E. R., Mayer, B., and Stuehr, D. J. (1997) *Biochemistry 36*, 10609−10619.
15. Abu-Soud, H. M., Gachhui, R., Raushel, F. M., and Stuehr, D. J. (1997) *J. Biol. Chem. 272*, 17349−17353.
16. Gorren, A. C. F., Bec, N., Schrammel, A., Werner, E. R., Lange, R., and Mayer, B. (2000) *Biochemistry 39*, 11763−11770.
17. Wu, C., Zhang, J., Abu-Soud, H., Ghosh, D. K., and Stuehr, D. J. (1996) *Biochem. Biophys. Res. Commun. 222*, 439−444.
18. Bradford, M. M. (1976) *Anal. Biochem. 72*, 248−252.
19. Sono, M., Ledbetter, A. P., McMillan, K., Roman, L. J., Shea, T. M., Masters, B. S. S., and Dawson, J. H. (1999) *Biochemistry 38*, 15853−15862.
20. Rusche, K. M., and Marletta, M. A. (2001) *J. Biol. Chem. 276*, 421−427.
21. Taylor, C. P. (1977) *Biochim. Biophys. Acta 491*, 137−148.
22. McMillan, K., and Masters, B. S. S. (1993) *Biochemistry 32*, 9875−9880.
23. Tierney, D. L., Huang, H., Martasek, P., Masters, B. S. S., Silverman, R. B., and Hoffman, B. M. (1999) *Biochemistry 38*, 3704−3710.

24. Chabin, R. M., McCauley, E., Calaycay, J. R., Kelly, T. M., MacNaul, K. L., Wolfe, G. C., Hutchinson, N. I., Madhusudanaraju, S., Schmidt, J. A., Kozarich, J. W., and Wong, K. K. (1996) *Biochemistry 35*, 9567−9575.
25. Salerno, J. C., Martasek, P., Roman, L. J., and Masters, B. S. S. (1996) *Biochemistry 35*, 7626−7630.
26. Spiro, T. G., and Li, X.-Y. (1988) in *Biological Applications of Raman Spectroscopy* (Spiro, T. G., Ed.) Vol. 3, pp 1−37, Wiley, New York.
27. Wang, J., Stuehr, D. J., Ikeda-Saito, M., and Rousseau, D. L. (1993) *J. Biol. Chem. 268*, 22255−22258.
28. Abu-Soud, H. M., Wang, J., Rousseau, D. L., and Stuehr, D. J. (1999) *Biochemistry 38*, 12446−12451.
29. Wang, J., Stuehr, D. J., and Rousseau, D. L. (1995) *Biochemistry 34*, 7080−7087.
30. Schelvis, J. P., Berka, V., Babcock, G. T., and Tsai, A. L. (2002) *Biochemistry 41*, 5695−5701.
31. Hu, S., Smith, K. M., and Spiro, T. G. (1996) *J. Am. Chem. Soc. 118*, 12638−12646.
32. Abu-Soud, H. M., Wu, C., Ghosh, D. K., and Stuehr, D. J. (1998) *Biochemistry 37*, 3777−3786.
33. Renodon, A., Boucher, J.-L., Wu, C., Gachhui, R., Sari, M.-A., Mansuy, D., and Stuehr, D. J. (1998) *Biochemistry 37*, 6367−6374.
34. Gerber, N. C., Rodriguez-Crespo, I., Nishida, C. R., and Ortiz de Montellano, P. R. (1997) *J. Biol. Chem. 272*, 6285−6290.
35. Gorren, A. C., Schrammel, A., Schmidt, K., and Mayer, B. (1997) *Biochemistry 36*, 4360−4366.
36. Boucher, J. L., Delaforge, M., and Mansuy, D. (1994) *Biochemistry 33*, 7811−7818.
37. Hart-Davis, J., Battioni, P., Boucher, J. L., and Mansuy, D. (1998) *J. Am. Chem. Soc. 120*, 12524−12530.
38. Wang, C., Ho, D., and Groves, J. T. (1999) *J. Am. Chem. Soc. 121*, 12094−12103.
39. Blumberg, W. E., and Peisach, J. (1971) in *Probes of Sructure and Function of Macromolecules and Membranes* (Chance, B., Yonetani, T., and Mildvan, A. S., Eds.) Vol. 2, pp 215−229, Academic Press, New York.
40. Dawson, J. H., Andersson, L. A., and Sono, M. (1982) *J. Biol. Chem. 257*, 3606−3617.
41. Sono, M., and Dawson, J. H. (1982) *J. Biol. Chem. 257*, 5496−5502.
42. Davydov, R., Ledbetter-Rogers, A., Martasek, P., Larukhin, M., Sono, M., Dawson, J. H., Masters, B. S. S., and Hoffman, B. M. (2002) *Biochemistry 41*, 10375−10381.

BI0272407